RSC Advances

PAPER

View Article Online
View Journal | View Issue

Cite this: *RSC Adv.*, 2020, **10**, 14089

Physicochemical and structural properties of lidocaine-based ionic liquids with anti-inflammatory anions†

Jovana Panić,[a] Aleksandar Tot,*[a] Nenad Janković,[b] Patrik Drid,[c] Slobodan Gadžurić[a] and Milan Vraneš[a]

Received 27th October 2019
Accepted 31st March 2020

DOI: 10.1039/c9ra08815f

rsc.li/rsc-advances

The purpose of this paper was to examine the density, viscosity and electrical conductivity at different temperatures, as well as the thermal stability and structural properties of previously reported ionic liquids based on active pharmaceutical ingredients. Lidocaine-based ionic liquids, with ibuprofen and salicylate as counterion, were prepared first. Their structures were confirmed by infrared, mass and ^{1}H and ^{13}C nuclear magnetic resonance spectroscopy. The Newtonian behaviour of lidocaine ibuprofenate was confirmed from viscosity measurement results, while it was impossible to determine for lidocaine salicylate. The interactions and structures of the studied ionic liquids were analyzed based on the measured density values, viscosity, electrical conductivity, and calculated values of thermal expansion coefficients and activation energy of viscous flow. From a theoretical aspect, DFT and MD calculations were performed. The obtained descriptors and radial distribution, as well as structural functions, were used to understand the structural organization of the synthesized ionic liquids.

Introduction

Over the last decade, ionic liquids (ILs), salts in the liquid form at or near room temperature, have captured much attention due to their large number of striking properties, such as low bioaccumulation, high thermal stability, designable nature, negligible vapour pressure, remarkable solvation abilities, good recyclability, and low toxicity.[1] Besides their unique properties, ILs can be considered as "tailored or designer solvents", because their physicochemical properties (*viz.* viscosity, density, conductivity, melting point, miscibility with other solvents) entirely depend on their structure, *i.e.* cation/anion selection. The ILs tunable nature expanded their use from the replacement of solvents and catalysts for synthesis to promising application in the pharmaceutical industry.[1,2] However, it is in the pharmaceutical and medical field that ILs have attracted particular attention since they can be used during the synthesis of drugs (as catalysts or reaction media, solvents/antisolvents, cosolvents), due to the possibility of forming additional interactions between the IL and the drug substance (like a hydrogen bond) and thus induce increased drug solubility.[2] Further, there has been growing interest of using ILs in drug delivery, as dispersing agents, copolymers or emulsifiers.[3] Nowadays, active pharmaceutical ingredients (APIs) are preparing in the form of ionic liquids (API-ILs) to maximize solubility, bioavailability, the concentration of the active ingredient(s), thermal stability, as well as to decrease the polymorphism of the drug.[2,4] Through the API-ILs synthesis, numerous possibilities to obtain any dual-function drug are opened, also. It also opens up the possibility to synthesize the desired dual function. It has become evident that ILs may be beneficial in the pharmaceutical area as these salts may be included in aqueous, oily or hydroalcoholic solutions, inducing increased drug solubility and/or enhanced topical and transdermal administration.

In this work, attention was dedicated to two API-ILs, lidocaine ibuprofenate ([Lid][Ibp]) and lidocaine salicylate ([Lid][Sal]). It is generally known that lidocaine has been using for local anaesthesia, while ibuprofen and salicylate are nonsteroidal anti-inflammatory drugs (NSAID). The combination of local anaesthetic and NSAID drugs has shown positive effects in the treatment of analgesia in animals.[5] In human practice, such formulations would find the most extensive use in the local treatment of acute pain and inflammation, with the most effortless topical application. To achieve these dual drug function, necessary is to modify or improve some of the physicochemical properties that these drug substances have while in solid form. By combining these drugs into the ionic liquid, certain problems induced by their structure properties, like low skin permeability for some NSAIDs, which limit their

[a]*Faculty of Science, Department of Chemistry, Biochemistry and Environmental Protection, University of Novi Sad, Trg Dositeja Obradovića 3, 21000 Novi Sad, Serbia. E-mail: aleksandar.tot@dh.uns.ac.rs*

[b]*Department of Chemistry, Faculty of Science, University of Kragujevac, Radoja Domanovića 12, 34000 Kragujevac, Serbia*

[c]*Faculty of Sport and Physical Education, University of Novi Sad, Lovćenska 16, 21000 Novi Sad, Serbia*

† Electronic supplementary information (ESI) available. See DOI: 10.1039/c9ra08815f

transdermal use, are overcome. Recently, studies about novel ILs with the potential anti-inflammatory application reported that transformation to an ionic liquid leads to the improved lipophilicity/hydrophilicity of drugs, and thus better permeability through a cell membrane compared with solid salts, lidocaine and ibuprofen.[6–9] In the literature, is still arguing if lidocaine ibuprofenate is an ionic liquid or deep eutectic salt. Although lidocaine ibuprofenate was first labelled as an ionic liquid and that term further expanded,[8,9] in the work of Berton *et al.*[7] it has been found as a deep eutectic liquid cocrystal with strong hydrogen bonds or interactions between partially ionized species. Lidocaine salicylate and acetylsalicylate have been prepared as dual-functional ILs also, but lidocaine acetylsalicylate showed limited stability due to conversion to salicylate.[10]

Altogether, both experimental and theoretical studies about structure, physicochemical properties, as well as studies on contacts between ILs and lipid membranes, remain rather popular. Although the number of new ionic liquids based on active pharmaceutical ingredients is rapidly rising, there is a lack of fundamental information about density, viscosity, electrical conductivity and thermal properties. Thus, this paper aims is to determine the physicochemical properties of earlier reported ionic liquids based on APIs, lidocaine ibuprofenate and lidocaine salicylate. Such study is significant when combined with complementary investigations, for developing and finding new active ingredients with improved pharmacokinetic characteristics.

Experimental

Apparatus and experimental procedures are described and given in ESI,† as well as the provenance and purity of used compounds (Table S1†).

The general procedure of lidocaine-based ionic liquids preparation

The preparation of lidocaine ibuprofenate and lidocaine salicylate was accomplished by mixing the appropriate amount of lidocaine with the appropriate equimolar amount (1 : 1) of ibuprofen/salicylic acid, dissolved in methanol, and stirred for 2 h at room temperature (Scheme 1). The remaining solvent was removed using a rotary evaporator on a temperature of 313.15 K. The light yellow lidocaine ibuprofenate, and colourless, viscous lidocaine salicylate, liquid at room temperatures with no tendency for crystallization during the work, were obtained. For the structure confirmations and the purities of the synthesized ILs, the IR, NMR, and MS spectra were recorded with appropriate assignation (Fig. S2–S5 in the ESI†). The obtained purity, calculated from NMR spectra, for lidocaine ibuprofenate amounts of 92.0% and lidocaine salicylate for 93.5%.

The IR spectrum data of synthesized lidocaine ibuprofenate and lidocaine salicylate, as well as spectra of lidocaine, salicylic acids and ibuprofen, was used to estimate the level of the conversion to ionic liquid (Fig. 1 in manuscript and Fig. S4–S6 in ESI†). This approach was successfully applied in determination of starting compounds conversion to lidocaine etodolac ionic liquid.[6] The wave numbers, ν (cm^{-1}) of the carbonyl groups in the carboxylic group of salicylic acid and ibuprofen, the carbonyl groups of amides in the lidocaine, the carbonyl groups of carboxylate anions ($-COO^-$) and the amides in the lidocaine salicylate and lidocaine ibuprofenate were compared. Thereby, the presence of obtained products in form of ionic liquids was concluded. The measured spectra were presented in Fig. S4–S6 in ESI,† while characteristic bands were presented in Table 1.

As can be seen from Table 1 and Fig. 1a, in lidocaine salicylate, the absorption bands characteristic to C=O stretching of the carboxyl group of salicylic acid were diminished (1658 cm^{-1}) and a new band appeared at about 1589 cm^{-1}. This provided evidence that salicylic acid is completely deprotonated in lidocaine salicylate, proving completely conversion to ionic liquid.

On the other hand, the C=O stretch in lidocaine ibuprofenate is located at around 1688 cm^{-1}, and present combination of three peaks (Fig. 1b). These peaks are located at 1664 cm^{-1} (C=O stretch of lidocaine amide group), 1720 cm^{-1}

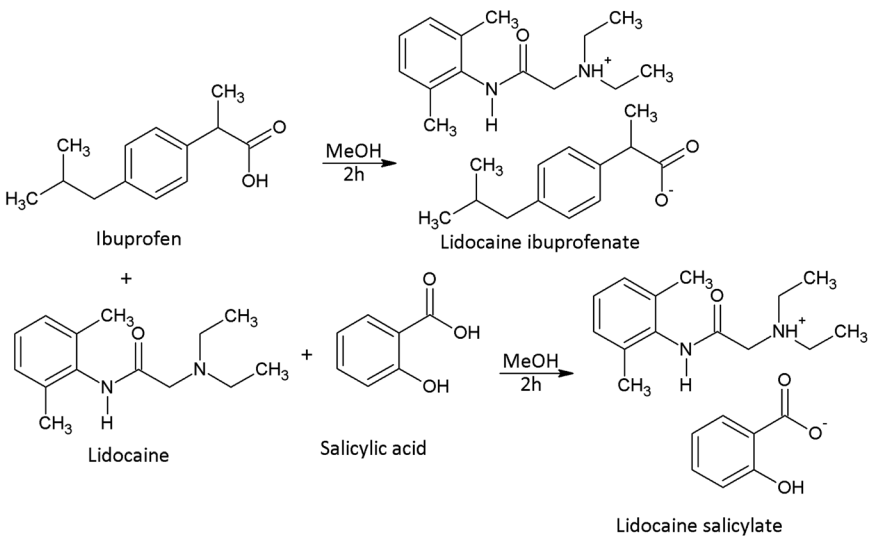

Scheme 1 Synthetic pathway of lidocaine ibuprofenate and lidocaine salicylate.

(C=O of ibuprofen) and a new broad peak at 1690 cm^{-1} which indicate a dynamic equilibrium between ibuprofene, lidocaine and H-bonded lidocaine ibuprofenate.[7] These observation suggest that ibuprofene is not completely in deprotonated state, indicating that conversion of lidocaine ibuprofenate in form of ionic liquid is not complete.

Results and discussion

Thermal analysis

The thermal stability of starting compounds and obtained ionic liquids, as well as phase transition values of obtained ionic liquids were determined by the thermogravimetric and DSC measurements and compared with results noted in earlier works.[8–11] In Fig. S1,† TG decomposition curves of the starting compounds and synthesized ionic liquids are presented. From Fig. S1,† it can be seen that the decomposition of ionic liquids starts at higher temperatures, which indicate that the conversion of starting components into ionic liquids increase the thermal stability of the compounds. Also, the number of decomposition stage of salicylic acid is reduced to one by conversion into lidocaine salicylate. The established decomposition onset temperatures (T_{onset}), 5% mass loss decomposition temperature ($T_{5\%\ onset}$), glass transition (T_g) and melting temperatures (T_m) are given in Table S2.† The obtained values of 5% mass loss decomposition and glass transition temperatures for lidocaine ibuprofenate and lidocaine salicylate are consistent with $T_{5\%\ onset}$, and T_g previously reported (See Table S2†).[8–11] Small deviations from the literature values are due to differently applied heating rates in the procedure of thermal analysis. Observing the obtained DSC thermograms (Fig. S1c and S1d†) the melting point above 100 °C of lidocaine salicylate was noted. Zürner *et al.*[12] explained this metastable liquid phase at room temperature as a glassy state of ionic liquids induced by the slow diffusion of the ions and insufficient crystal nucleation during cooling of a system. In earlier work, the melting point for lidocaine salicylate was not observed, as, during the DSC measurement, the sample was heated only up to 110 °C.

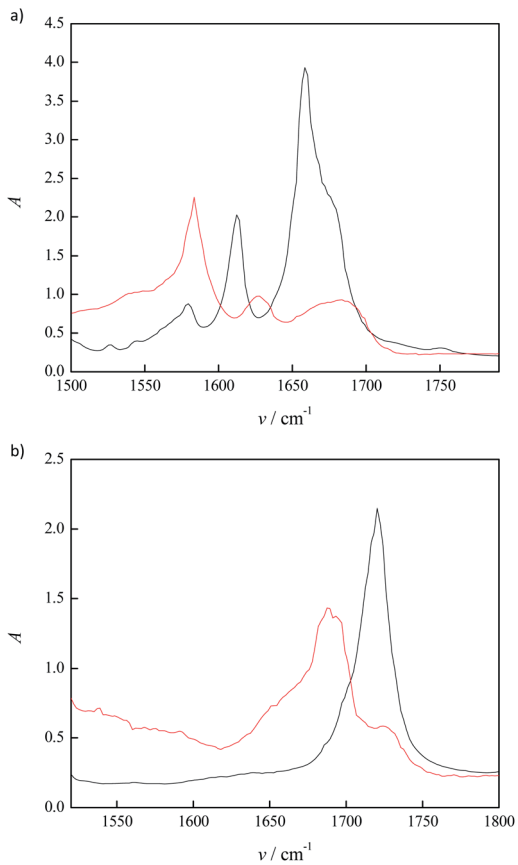

Fig. 1 The IR spectra in region of 1500–1800 cm^{-1} for: (a) lidocaine salicylate (red) and salicylic acid (black); (b) lidocaine ibuprofenate (red) and ibuprofene (black). The absorbance values of ionic liquids are multiplied with factor 5 for easier comparation.

Density

The densities (d) of pure lidocaine ibuprofenate were measured in the temperature range from $T = (293.15$ to $323.15)$ K, while of pure lidocaine salicylate from $T = (318.15$ to $353.15)$ K at atmospheric pressure ($p = 0.1$ MPa). The density of lidocaine salicylate could not be measured below $T = 318.15$ K by applied instrument due to the high viscosity of the pure ionic liquid.

The thermal expansion coefficients for the pure ILs, α_p, was calculated from obtained experimental densities:

$$\alpha_p = -\frac{1}{d}\left(\frac{\partial d}{\partial T}\right)_{p,m}$$

The thermal expansion coefficient was determined in the same temperature range as measured densities. The obtained results are tabulated in Tables 2 and 3 and graphically shown as a variation with temperature, in Fig. 2 for d and Fig. 3 for α_p.

By virtue of the fact that the density of ILs dependent upon directly on cation–anion interaction, it can be concluded that denser lidocaine salicylate has a better geometric fit of planar aromatic systems and stronger stabilization π–π interactions existence between lidocaine and salicylate than between lidocaine and ibuprofenate.[13] Additionally, a higher thermal expansion coefficient of lidocaine ibuprofenate evidenced a faster movement of the cation from the anion, due to weaker interactions between them.

Viscosity

The viscosity measurements were performed in temperature range from $T = (293.15$ to $323.15)$ K for lidocaine ibuprofenate

Table 1 IR absorption bands for characteristic vibrations

Compound	Assignment	Wave number (cm^{-1})
Salicylic acid	–COOH	1658
Ibuprofene	–COOH	1720
Lidocaine salicylate	$–COO^-$	1589
Lidocaine ibuprofenate	$–COO^-$	1688

Table 2 Experimental densities (d), viscosities (η), electrical conductivities (k), calculated molar conductivities (λ_m), and thermal expansion coefficients (α_p) of lidocaine ibuprofenate at different temperatures

T/K	d^a/g cm^{-3}	η^b/mPa s	$k^b \times 10^4$/mS cm^{-1}	$\lambda_m \times 10^4$/S cm^2 mol^{-1}	$\alpha_p \times 10^4$/K^{-1}
293.15	1.02546	20 712	1.44	0.62	8.28
298.15	1.02145	5606.9	2.51	1.08	8.32
303.15	1.01715	2806.0	4.75	2.06	8.35
308.15	1.01278	1467.6	7.48	3.26	8.39
313.15	1.00860	832.08	12.5	5.47	8.42
318.15	1.00436	468.49	18.1	7.95	8.46
323.15	1.00006	298.75	28.1	12.4	8.49

^{a} Standard uncertainty: $u(d) = 3.0 \times 10^{-3}$g cm^{-3}, $u(T) = 0.015$ K. ^{b} Relative standard uncertainty: $u_r(\eta) = 0.02$, $u_r(k) = 0.01$.

and from $T = (298.15$ to $353.15)$ K for lidocaine salicylate. The obtained results are given in Tables 2 and 3.

Variation of viscosity with temperature was fitted using the Vogel–Fulcher–Tammann (VFT) equation[14–16] (Fig. 4):

$$\eta = A \exp\left(\frac{B}{T - T_g}\right)$$

A and B are adjustable parameters. T_g represents glass transition temperature. The fitting parameters are given in Table S3.†

The determination of Newtonian or non-Newtonian behaviour was applied for lidocaine ibuprofenate, while for lidocaine salicylate it was impossible. Namely, for determination of Newtonian behaviour the measurements with a wide range of RPM are necessary. Unfortunately, due to the high viscosity of lidocaine salicylate and the limitation of equipment at higher RPM measurements with LV-4 spindle were impossible. The viscosity of fluids with Newtonian behaviour at a given temperature remains constant regardless of which Viscometer model, spindle or speed was used for the measurements. A linear dependency of shear stress from shear rate presented in Fig. 5 (Table S4†), together with the constant viscosity with shear rate values indicate Newtonian behaviour of lidocaine ibuprofenate.

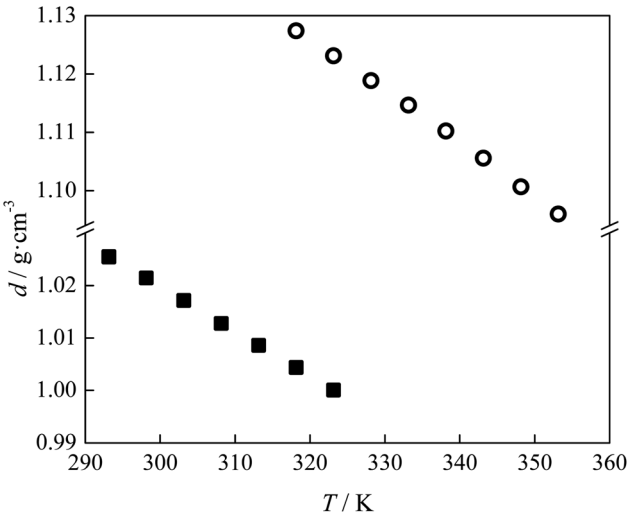

Fig. 2 Variation of: ■ lidocaine ibuprofenate, and ○ lidocaine salicylate density with temperature.

Electrical conductivity

The electrical conductivity of lidocaine ibuprofenate was measured in the temperature range from $T = (293.15$ K to

Table 3 Experimental densities (d), viscosities (η), electrical conductivities (k), calculated molar conductivities (λ_m), and thermal expansion coefficients (α_p) of lidocaine salicylate at different temperatures

T/K	d^a/g cm^{-3}	$\eta^b \times 10^{-4}$/mPa s	$k^b \times 10^4$/mS cm^{-1}	$\lambda_m \times 10^4$/S cm^2 mol^{-1}	$\alpha_p \times 10^4$/K^{-1}
298.15	—	5836.9	—	—	—
303.15	—	1483.1	—	—	—
308.15	—	290.52	—	—	—
313.15	—	89.149	0.40	—	—
318.15	1.12741	29.004	1.75	0.57	8.10
323.15	1.12311	10.226	5.62	1.84	8.13
328.15	1.11885	5.0573	12.6	4.16	8.17
333.15	1.11468	2.2890	29.0	9.57	8.20
338.15	1.11025	0.9496	61.8	20.5	8.23
343.15	1.10558	0.4308	116	38.6	8.26
348.15	1.10065	0.1809	209	70.0	8.30
353.15	1.09597	0.0970	349	118	8.34

^{a} Standard uncertainty: $u(d) = 3.0 \times 10^{-3}$g cm^{-3}, $u(T) = 0.015$ K. ^{b} Relative standard uncertainty: $u_r(\eta) = 0.02$, $u_r(k) = 0.01$.

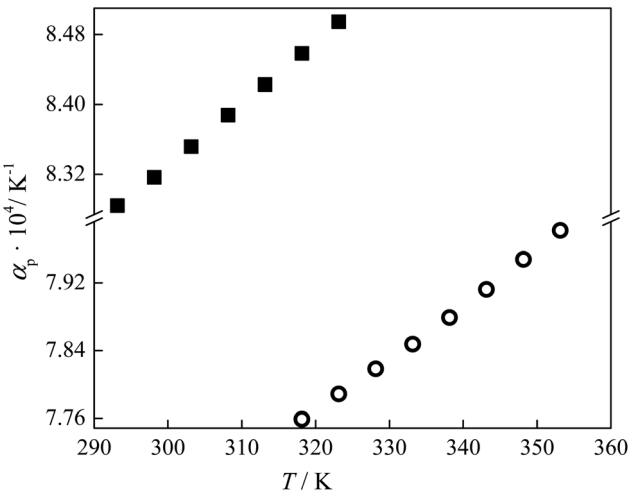

Fig. 3 Variation of thermal expansion coefficients of ILs with temperature: ■ lidocaine ibuprofenate, and ○ lidocaine salicylate.

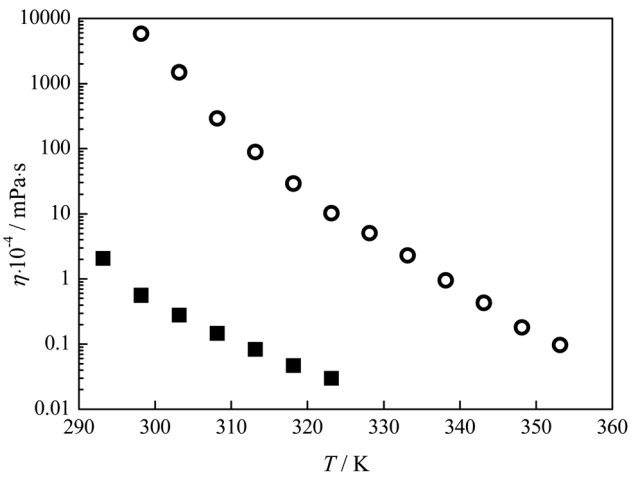

Fig. 4 Variation of viscosity with temperature for pure ionic liquids: ■ lidocaine ibuprofenate, and ○ lidocaine salicylate.

323.15 K), while for lidocaine salicylate in the range from $T =$ (313.15 K to 353.15 K). The measured values are presented in Tables 2 and 3 The variation of electrical conductivity with

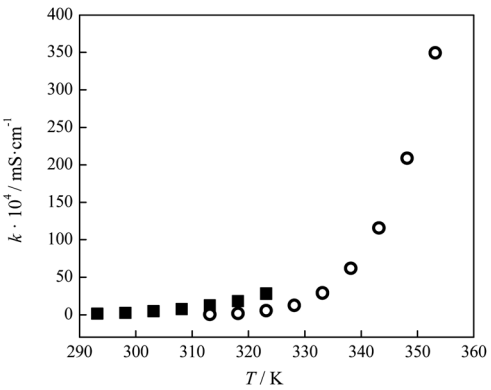

Fig. 6 Variation of electrical conductivity of pure ionic liquids with temperature: ■ lidocaine ibuprofenate, and ○ lidocaine salicylate.

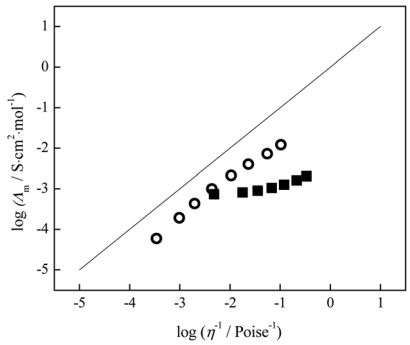

Fig. 7 Walden plot for lidocaine ibuprofenate, ■, in temperature range 293.15–323.15 K, and lidocaine salicylate, ○, in temperature range 318.15–353.15 K.

temperature is shown in Fig. 6, and fitted using modified VFT equation:

$$\kappa = A' \exp\left(\frac{-B'}{T - T_g}\right)$$

A' is the pre-exponential coefficient, B' is the pseudoactivation energy and T_g is the ideal glass transition temperature. The fitting parameters are given in Table S5.† The values of molar

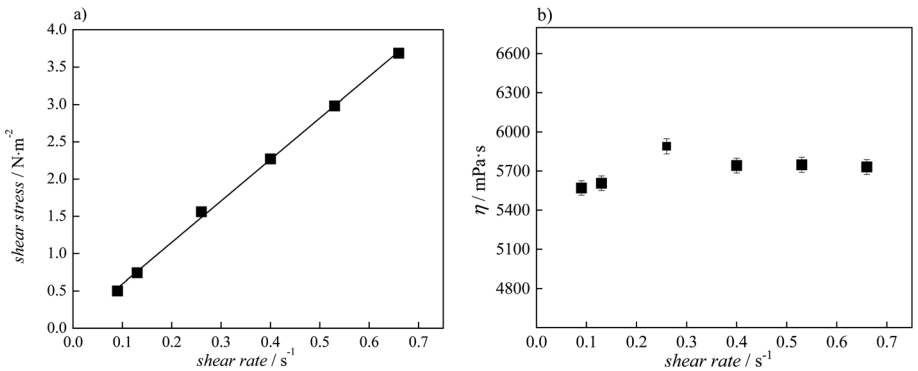

Fig. 5 (a) Flow curve, showing shear stress as a function of shear rate for pure lidocaine ibuprofenate; (b) changes of viscosity values at 298.15 K with shear rate along with error bars.

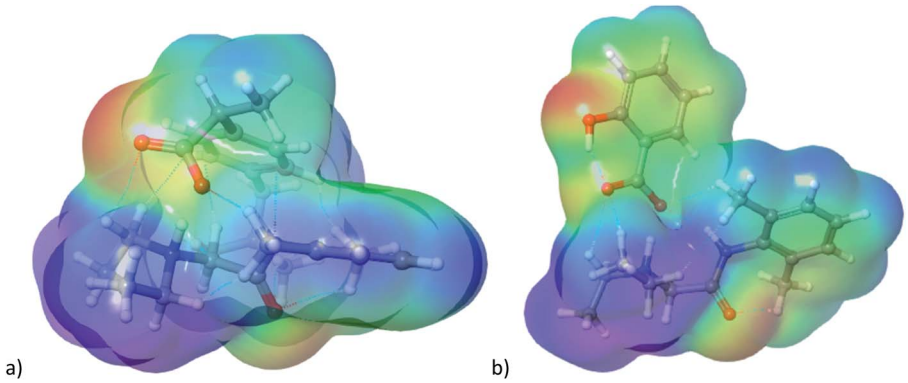

Fig. 8 Representation of MEP surfaces: (a) lidocaine ibuprofenate, (b) lidocaine salicylate.

conductivity (λ_m) were calculated from electrical conductivity using relation:

$$\lambda_m = \frac{\kappa}{c}$$

and obtained results are presented in Tables 2 and 3.

To predict ionicity for lidocaine salicylate and lidocaine ibuprofenate, Walden plot was applied.

The relation between molar conductivity and viscosity can be demonstrated by the equation:

$$\log \lambda_m = \log C + \alpha \log \eta^{-1}$$

where λ_m is molar conductivity, η^{-1} is fluidity, α is the slope of the line in the Walden plot which reflects the decoupling of the ions, C "is Walden product of fractional Walden rule". The Walden plot is presented in Fig. 7.

In the comparison of ideal KCl line, it can be seen that lidocaine salicylate and lidocaine ibuprofenate lie below this line. Further, the lidocaine salicylate is closer to KCl line, indicating better ionicity compared to lidocaine ibuprofenate. Typically, data for ionic liquids fall below this ideal line because of the strong interaction between ions in the pure ionic medium, which reduce the movement of most ions that are partially correlated with their closest neighbours. The traditional Walden plot shows three distinct groups of ionic liquids that are distinguished based on vertical distance to the KCl line, denoting as ΔW.[17] The first group lies quite close to the KCl line ($0.1 < \Delta W < 0.5$) suggesting that the ionic liquid is made up of almost independently mobile ions and can be classified as good ionic liquids.[17–19] The second groups lies lower on the plot ($0.5 < \Delta W < 1.0$) and is named "poor" ionic liquids. In this group existence of H-bonds and other specific interaction between ions in the pure state is more pronounced, leading to a significant reduction of ions mobility. The third group represents the liquids that are at least an order of magnitude below the ideal line, also described as liquid ion pairs or subionic liquids ($\Delta W > 1.0$).[17–19] In these liquids, ion conductivity is substantially less than would be expected based on their viscosity. The simplest example is the ion pair, which is neutral and therefore, does not contribute at all to the measured conductivity.

From Table 3 it can be seen that lidocaine salicylate, although being more viscous (290 Pa s) than lidocaine ibuprofenate (0.5 Pa s) nonetheless has similar conductivity, presumably because the degree of ion association is lower for lidocaine salicylate. This assumption is confirmed using Walden plot, where lidocaine salicylate is closer to idel KCl line ($\Delta W = 0.71$) and can be classified as "poor" ionic liquid. On the other side, lidocaine ibuprofenate lies in region of subionic liquids ($\Delta W = 1.34$) proving the predominance of ion pairs in its structure. This result is in accordance with conclusions driven

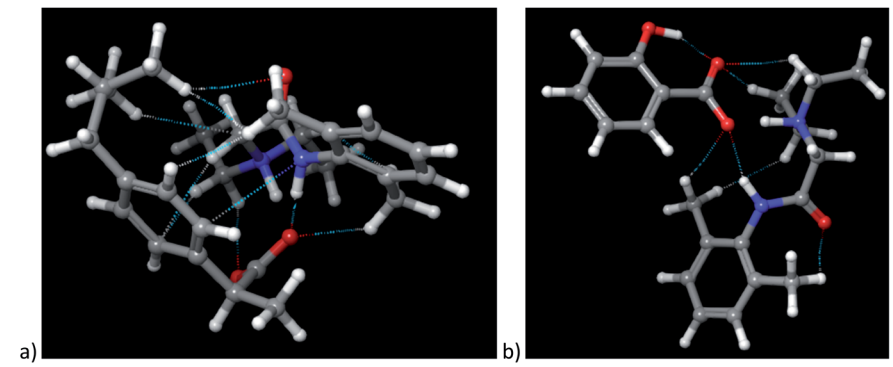

Fig. 9 Representation of optimized structures along with visualization of non-covalent interactions: (a) lidocaine ibuprofenate, (b) lidocaine salicylate.

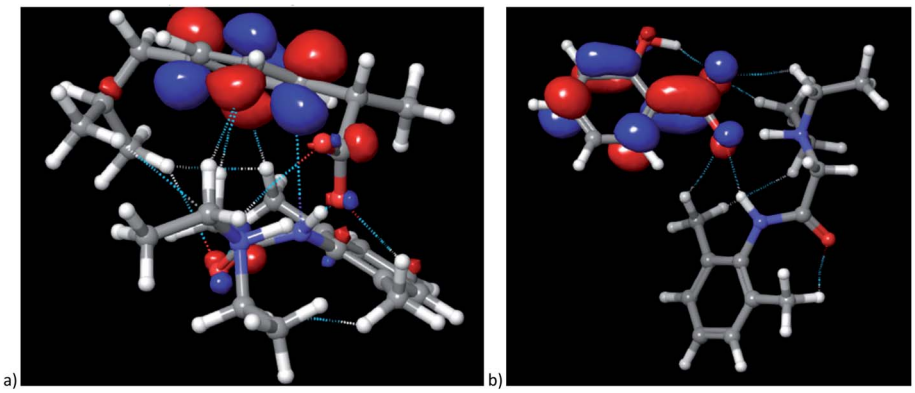

Fig. 10 Representation of LUMO orbitals: (a) lidocaine ibuprofenate, (b) lidocaine salicylate.

from FTIR measurements, proving that conversion of lidocaine ibuprofenate in classical ionic liquid is not fully accomplished.

Computational simulations

The cation–anion interactions in ionic liquids systems are determined by electrostatic properties of constituting ions, van der Waals interactions and the geometrical fitting of cation and anion. Thus, one of the useful descriptor for potential interaction sites is molecular electrostatic potential (MEP). In Fig. 8 the MEP surfaces for lidocaine ibuprofenate and lidocaine salicylate are presented. The negative regions of the molecular electrostatic potential are represented in red colour and are connected with the region of a molecule with the highest electrophilic reactivity. On the other hand, the blue regions represent the positive regions with pronounced nucleophilic reactivity. The negative electrostatic potential is located around oxygen atoms from cation and both anions. On the other hand, positive electrostatic potential is clearly positioned around methyl and $-NH^{+}$ groups of lidocainium cation, and as well as around amid nitrogen of cation. The negative electrostatic potential of C═O and positive on the –NH group of cation indicates a significant contribution of the resonant form of the peptide bond in which the nitrogen is positive, and the oxygen is negatively charged, preventing the free rotation around the C–N bond, and induces increase the structural rigidity of the molecule. In addition, in the case of ibuprofenate it can be noted the existence of positive potential around alkyl chain, which is absent for salicylate. The presence of both positive and negative electrostatic potential in the structure of cation, as well as in the case of ibuprofenate anion, leads to possible lidocaine–lidocaine and ibuprofenate–ibuprofenate interaction. With this purpose, the non-covalent interactions (NCI) from optimized monomer structure were presented in Fig. 9. As can be seen from Fig. 9, lidocaine ibuprofenate have significantly more NCI, suggesting stronger interactions between cation and anion, as it proved from Walden plot and FTIR measurements.

In addition, from Fig. 9 a potential intramolecular interaction between the keto group of lidocaine and the methyl group from the ortho position can be seen, which occurs as a result of

Table 4 The Values of HOMO–LUMO energy gap (ΔE_{gap}) for selected ionic liquids

Ionic liquid	ΔE_{gap}/eV
Lidocaine ibuprofenate	5.76
Lidocaine salicylate	4.95

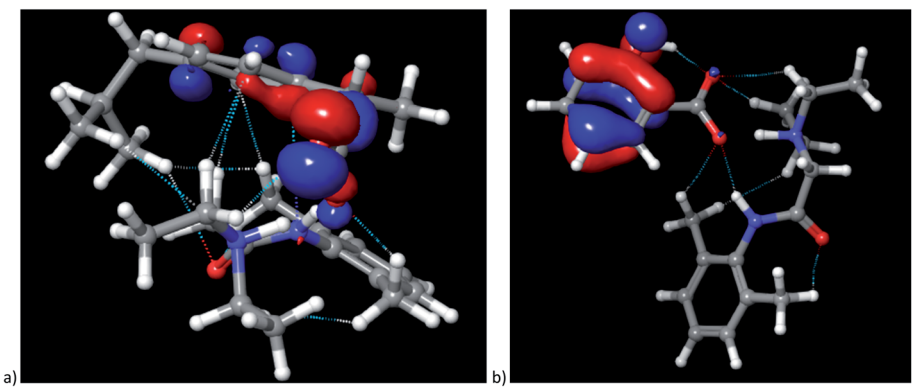

Fig. 11 Representation of HOMO orbitals: (a) lidocaine ibuprofenate, (b) lidocaine salicylate.

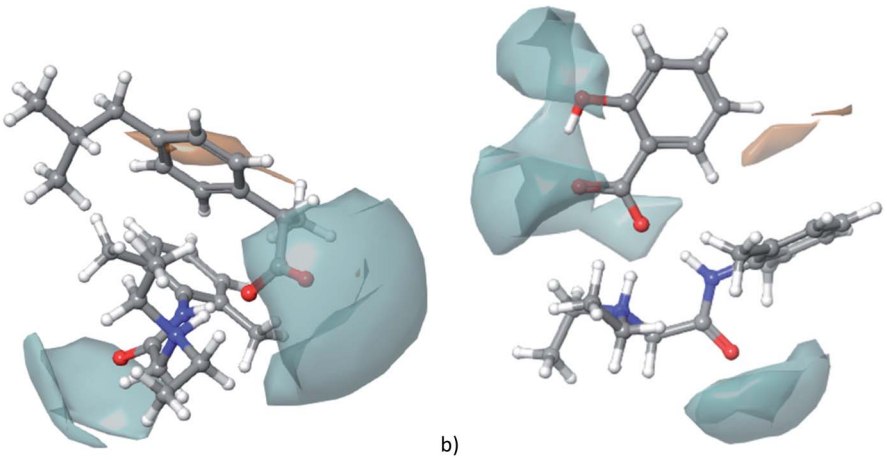

Fig. 12 Representation of hydrophilic (turquoise colour) and hydrophobic (orange colour) for investigated ionic liquids: (a) lidocaine ibuprofenate, (b) lidocaine salicylate.

Table 5 The values of *A* log *P* along with the percentage of hydrophilic surfaces obtained from DFT calculations of selected ionic liquids

Ionic liquid	*A* log *P*	Percentage of hydrophilic surfaces (%)
Lidocaine ibuprofenate	3.97	36.96
Lidocaine salicylate	1.55	46.83

an increase in the acidity of hydrogen atoms from the methyl group due to the expressed positive inductive and hyperconjugation effect, indicating the potential cation–cation interactions.

The next step was an analysis of frontier molecular orbitals (HOMO and LUMO) as a convenient tool for visualization of the global stability and reactivity of investigated compounds. The atomic contribution to HOMO–LUMO orbitals were generated and presented in Fig. 10 and 11 (positive electron density represents red colour and negative is in blue colour). From mentioned figures, in both ionic liquids, the HOMO and LUMO orbitals are mostly located above anions. The HOMO and LUMO orbitals shows which part of molecule had potential to interact with other structures, while the HOMO–LUMO difference represents the descriptor of this molecule stability. The HOMO and LUMO energy gap, ΔE_{gap} (Table 4), quantify the possible charge transfer interactions within the molecule. The smaller value of band ΔE_{gap} is connected to increased reactivity of the molecule. As can be seen in Table 4, the ΔE_{gap} is lower for lidocaine salicylate. Based on this observation lidocaine ibuprofenate is more stable IL implying lower chemical reactivity because it hinders electrons to high-lying LUMO or extracting electrons from a low-lying HOMO inhibiting the formation of an activated complex for any further reaction.

Further, hydrophobic/hydrophilic surfaces for both ionic liquids were calculated and presented in Fig. 12. Moreover, the percentage of hydrophilic surfaces, as well as lipophilic descriptor *A* log *P*, were calculated and shown in Table 5.

As can be seen from Table 5, both descriptors indicate that lidocaine salicylate is more hydrophilic than lidocaine ibuprofenate.

The molecular dynamic simulations were applied in order to obtain detailed information about global structure and interactions of pure ionic liquids. The using of MD simulations offers the opportunity to predict physical properties directly from a molecular interaction model and also to visualize the organization of molecules and their structure at a molecular level. This method was refined to present the position of a given ion corresponding to the position of the selected counterion, describing the local structure around ions using the structural analysis tools like radial distribution functions (RDFs) and structural factor calculations (SDFs).

The information about the distance between cations and anions were obtained from MD simulations using radial distribution function (RDFs). RDFs for anion (oxygens from COO^-) and hydrogens from N1 and N2 in all ionic liquids are presented in Fig. 13. From Fig. 13, it can be seen higher values of *g*(r) at a smaller distance for lidocaine salicylate. This behaviour indicates that salicylate, due to a smaller size, can approach closer to lidocainium cation, than more bulk ibuprofenate. This result, indicate better, denser packaging of smaller salicylate between lidocainium cations, causing higher values of density and viscosity of lidocaine salicylate comparing to lidocaine ibuprofenate. The lidocaine ibuprofenate with branched, more hydrophobic tail prevents packaging of the ions and decrease the efficiency of π–π interactions more than salicylate. These results are in accordance with lower T_g values and higher conductivity of lidocaine ibuprofenate.

Further, comparing results for hydrogen attached to N1 and N2 atoms, it can be seen that hydrogen connected to N2 is closer to both anions. On the other hand, this makes N1 atom of lidocaine more available for additional interaction. With this purpose, the RDFs between N1 and O1 atom from lidocaine cation were calculated and shown in Fig. 14, to present the possibility of self-aggregation of lidocaine cation. From Fig. 14, the significant peak at 2.8 Å is noted, suggesting the self-

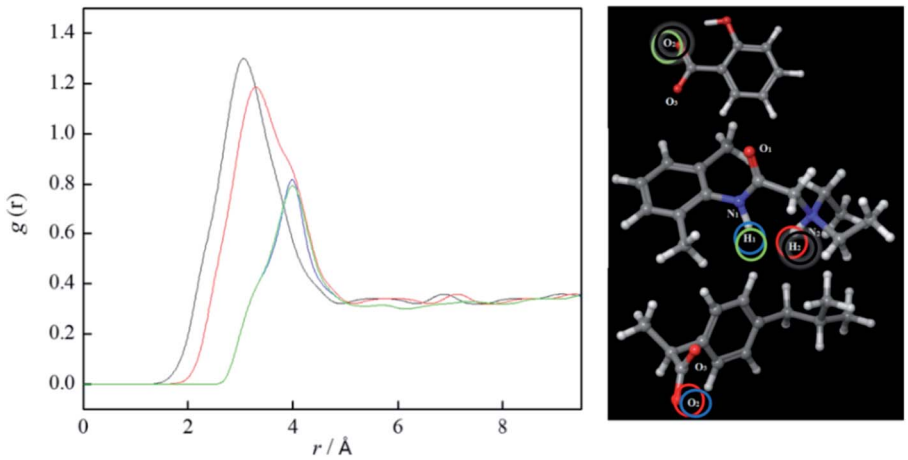

Fig. 13 The RDFs of selected atoms from anion and cations (red line O2 and H2 from lidocaine ibuprofenate, blue line O2 and H1 from lidocaine ibuprofenate, black line O2 and H2 from lidocaine salicylate, green line O2 and H1 from lidocaine salicylate).

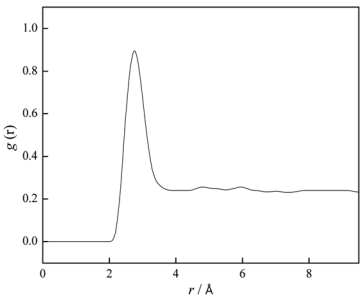

Fig. 14 The RDF of O1 and H1 from lidocaine ibuprofenate.

aggregation tendency of lidocaine due to possible formation of H-bond between N1 and O1 atoms of lidocaine.

To separate anionic and cationic contributions to RDFs, structure functions were calculated for the representative centre of cation's, and anion's center of mass and results are presented in Fig. 15. As can be seen from Fig. 15, the same contribution of cation–cation and cation–anion to interaction in pure ionic liquid were obtained. The only differences are in anion–anion interactions, where the negative contribution to structure factor is noted in lidocaine salicylate, which is in contrary to lidocaine ibuprofenate. All obtained theoretical results indicate that ibuprofenate have a tendency to interact with itself, creating more cluster structures comparing to salicylates where this type of interactions are absent. The existence of anion segregation in lidocaine ibuprofenate originates from the partially deprotonated carboxylic group, which diminish electrostatic repulsion between negative charged anions, allowing the formation of H-bond between protonated and deprotonated $-COO^{-}$ group of ibuprofen. As the last evidence of stronger interactions between cation and anion in lidocaine salicylate, the ion pair binding energy (ΔG_{bin}) was calculated. This is important parameter that can be correlated with physico-chemical properties of ILs such as melting point, thermal stability and transport properties.[20] The significantly more negative energy was obtained for lidocaine salicylate ($E_{bin} = -116.21$ kJ mol^{-1}) than for lidocaine ibuprofenate ($E_{bin} = -71.44$ kJ mol^{-1}). From work of Bernard *et al.* and from obtained experimental results in this work, the dependence between low value of ΔG_{bin} and higher values of viscosity and density were obtained.[21] This confirms that ion pair binding energy is correlated with the strength of the intermolecular interaction between ions. Lower value of

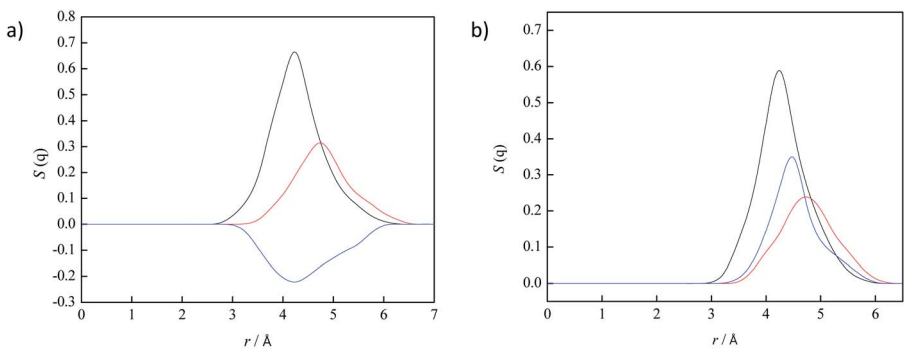

Fig. 15 Partitioning of $S(q)$ to cation–cation (red line), cation–anion (black line) and anion–anion (blue line) correlations: (a) lidocaine ibuprofenate, (b) lidocaine salicylate.

binding energy points to stronger molecular packaging, suggesting higher value of density and viscosity, as in the case of investigated ionic liquids.

Conclusions

Given the growing interest in ionic liquids based on active pharmaceutical ingredients, this study was conducted to obtain a physicochemical and structural characterization of previously reported lidocaine-based ionic liquids with anti-inflammatory anions. In that intent, lidocaine ibuprofenate and lidocaine salicylate were synthesized, and their structures were verified by IR, MS, and NMR spectra. Thermal, densimetric, viscosimetric, and electrical conductivity measurements were performed, supported by DFT calculations and molecular dynamics simulation. Thermal analysis has shown that by the synthesis of ionic liquids, more thermally stable compounds were obtained relative to the starting components. From experimental and theoretical results, the better, denser packaging of smaller salicylate between lidocainium cations, was noted, inducing higher values of density and viscosity, and lower electrical conductivity of lidocaine salicylate comparing to lidocaine ibuprofenate. From DFT calculations and MD simulations, the more pronounced interactions between lidocaine and salicylate were suggested. The obtained RDFs and structural factor analysis indicate that in lidocaine ibuprofenate existed anion segregation while in lidocaine salicylate this type of interactions is absent.

Conflicts of interest

Authors have no any conflict of interest to declare.

Acknowledgements

This work was financially supported by the Ministry of Education, Science and Technological Development of the Republic of Serbia under project contract ON172012.

References

1 G. Rohitkumar and N. Gathergood, Safer and greener catalysts – Design of high performance, biodegradable and low toxicity ionic liquids, in *Ionic Liquids – New Aspects for the Future*, ed. J. Kadokawa, IntechOpen, London, 2013, pp. 499–535.
2 R. T. Ley and A. S. Paluch, *J. Chem. Phys.*, 2016, **144**(8), 084501.
3 N. Adawiyah, M. Moniruzzaman, S. Hawatulailaa and M. Goto, *Med. Chem. Commun.*, 2016, **7**, 1881–1897.
4 K. Egorova, E. Gordeev and V. Ananikov, *Chem. Rev.*, 2017, **117**, 7132–7189.
5 M. S. Herskin and B. H. Nielsen, *Front. Vet. Sci.*, 2018, **5**(117), 1–16.
6 Y. Miwa, H. Hamamoto and T. Ishida, *Eur. J. Pharm. Biopharm.*, 2016, **102**, 92–100.
7 P. Berton, K. R. Di Bona, D. Yancey, S. A. A. Rizvi, M. Gray, G. Gurau, J. L. Shamshina, J. F. Rasco and R. D. Rogers, *ACS Med. Chem. Lett.*, 2017, **8**, 498–503.
8 H. Wu, Z. Deng, B. Zhou, M. Qi, M. Hong and G. Ren, *J. Mol. Liq.*, 2019, **283**, 399–409.
9 H. J. Park and M. R. Prausnitz, *AIChE J.*, 2015, **61**, 2732–2738.
10 K. Bica, C. Rijksen, M. Nieuwenhuyzen and R. D. Rogers, *Phys. Chem. Chem. Phys.*, 2010, **12**, 2011–2017.
11 K. Bica, H. Rodríguez, G. Gurau, O. A. Cojocaru, A. Riisager, R. Fehrmannd and R. D. Rogers, *Chem. Commun.*, 2012, **48**, 5422–5424.
12 P. Zürner, H. Schmidt, S. Bette, J. Wagler and G. Frisch, *Dalton Trans.*, 2016, **45**, 3327–3333.
13 M. Vraneš, J. Panić, A. Tot, M. Popsavin, A. Jocić and S. Gadžurić, *J. Chem. Thermodyn.*, 2019, **131**, 80–87.
14 H. Vogel, *Phys. Z.*, 1921, **22**, 645–646.
15 G. S. Fulcher, *J. Am. Ceram. Soc.*, 1925, **8**, 339–355.
16 G. Tammann and W. Hesse, *Z. Anorg. Allg. Chem.*, 1926, **156**, 245–257.
17 D. R. Macfarlane, M. Forsyth, E. I. Izgorodina, A. P. Abbott, G. Annat and K. Fraser, *Phys. Chem. Chem. Phys.*, 2009, **11**, 4962–4967.
18 K. R. Harris, *J. Phys. Chem. B*, 2019, **123**, 7014–7023.
19 K. J. Fraser, E. I. Izgorodina, M. Forsyth, J. L. Scott and D. R. MacFarlane, *Chem. Commun.*, 2007, 3817–3819.
20 H. Roohi and S. Khyrkhah, *J. Mol. Model.*, 2013, **21**, 1–11.
21 U. L. Bernard, E. I. Izgorodina and D. R. MacFarlane, *J. Phys. Chem. C*, 2010, **114**, 20472–20478.